PRNC 58

PUERTO RICO NUCLEAR CENTER

RADIATION DAMAGE IN ORGANIC CRYSTALS

Progress Summary Report No. 3

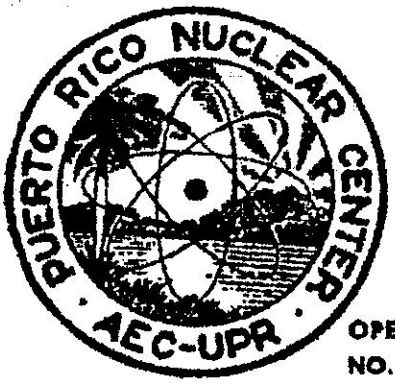

OPERATED BY UNIVERSITY OF PUERTO RICO UNDER CONTRACT
NO. AT (40-1)-1833 FOR U. S. ATOMIC ENERGY COMMISSION

STUDY OF RADIATION DAMAGE IN ORGANIC CRYSTALS USING ELECTRICAL CONDUCTIVITY

Amador Cobas, H. Harry Szmant, Alfredo J. Torruella, Seymour Trester and Zvi Weisz - Principal Investigators

Progress Report #3

Work performed at Puerto Rico Nuclear Center
Rio Piedras, P.R., under U. S. Atomic Energy
Commission Contract AT(40-1)-1833 (Project 14)

January 1965

TABLE OF CONTENTS

INTRODUCTION:

This project is concerned with the effects of radiation on organic crystals. It is felt that such studies on well defined crystalline structures can provide a firm foundation for a later study of more complex materials including those of direct biological interest. We have chosen anthracene as the initial material for study because this substance has been studied more than any other organic material.

The effect of neutron irradiation on anthracene has been studied previously by Kommandeur[1,2], but to the best of our knowledge, no other work on this subject has appeared since then. Since Kommandeur's work was done very early in the history of organic conductivity, we felt that it would be valuable to reopen and expand this work to include more recent developments such as the introduction of charge-injecting electrodes [3], and the application of space-charge-limited current theory to molecular crystals[4,5,6,7,8,9,10,11,12].

Below is a summary of the results obtained during the period January 1964 to December 1964.

Our preliminary results of neutron radiation damage presented in our Progress Reports #1 and #2 indicated that in electrical conductivity measurements a change in the saturation current occurs after a very low dose of radiation. These measurements were made using a Kallmann-Pope[13] cell with Na_2SO_4 solution as one of the electrodes and $NaI-I_2$ solution as the hole injecting electrode. Subsequent measurements with a more sensitive electrode system recently developed at our laboratory indicate that the

changes detected are most likely an electrode effect rather than a change in the crystal itself. However, our most recent work shows that after irradiating with gamma rays or x-rays and making the measurements with the improved electrode system a definite change in the electrical conductivity of the crystals is detected while no change was observed after neutron irradiation of doses comparable to those reported previously. These results comprise the main part of this report.

SECTION I. CRYSTALS

As discussed in Summary Report #2 we have used an improved Kallmann-Pope[14] technique to grow large anthracene crystals from solution. The main features of this technique is to use a solvent comprised of equal parts by volume of dichlorethane, cis-dichloroethylene and trans-dichloroethylene and to carefully control the rate of cooling of the solution. A complete description of this technique will be submitted for publication in the near future.

Using this technique we have grown all the crystals needed for our experiment. These crystals, because of their large area (approximately 2 cm^2), and appropriate thickness which ranges from 20 to 100 microns, were especially suited for our measurements.

SECTION II. IRRADIATION PROCEDURES

Crystals were irradiated using the following radiation sources:

(a) a Pu-Be neutron source
(b) the thermal column at the PRNC research reactor
(c) a Co-60 gamma cell
(d) a 120 kvp x-ray radiotherapy unit

Our Pu-Be neutron source is a 10 curie source imbedded in paraffin. The crystals were placed right next to the source where the flux is approximately 2×10^5 n cm^{-2} sec^{-1} and the average neutron energy is approximately 2 Mev. Assuming the neutron absorption coefficient of anthracene to be approximately equal to that of similar organic substances the neutron radiation absorbed by anthracene is approximately 3×10^{-9} rads/n/cm^2[15] where 1 rad equals 100 ergs/gm. Due to the fact that our Pu-Be neutron source has such a small flux the doses given in reasonably short times (3 days to 1 week) were of the order of a few rads.

The crystals irradiated with the reactor were irradiated with thermal neutrons (.025 ev). The flux used was approximately 10^9 n/cm^2/sec and the doses given ranged from 1000 to 12,000 rads approximately.

The Co-60 gamma cell used to irradiate our crystals has an output of 780 r/min. and the energies of the Co-60 photons are 1.33 and 1.17 Mev. By measuring the absorption coefficient of anthracene for the Co-60 photons, which turned out to be 0.118 cm^{-1}, we calculated that the energy absorbed by anthracene is 293 ergs gm^{-1} r^{-1}. The doses given ranged from 8×10^2 to 10^6 r.

The x-ray unit used to irradiate our crystals was a 120 kvp radiotherapy unit with an output of 335 r/min. By measuring the absorption coefficient of anthracene for this radiation, which turned out to be 0.671 cm^{-1}, we calculated that the energy absorbed by anthracene is 296 ergs gm^{-1} r^{-1}. The doses given ranged from 8×10^2 r to 10^6 r.

SECTION III. EXPERIMENTAL SET UP

The experimental set-up is shown in Fig. 1. The electrode configuration system that we have developed and used is as follows. The non-injecting electrode consists of a piece of transparent conducting glass (evaporated tin oxide on one of the surfaces) on which a small drop of 1M Na_2SO_4 solution is placed. The crystal is then layed on top of the Na_2SO_4 solution drop which then spreads producing a very good electrical contact between the crystal and the conducting glass. The injecting electrode on the opposite side of the crystal consists of a drop of NaI-I_2 solution into which a platinum wire is inserted and held in place by a simple insulated support. In order that the reproducibility of the saturation value of the current be within a factor of two, the concentration of the I_2 in the NaI-I_2 solution has to be within well defined limits. This concentration is achieved by diluting a saturated solution of iodine in 1M NaI at room temperature to 25-50% dilution. With a saturated solution the

reproducibility of the saturation current values is very poor.

Voltages between 2 and 500 volts were applied to the crystals from a Keithley Model 240 regulated power supply. The currents were measured using a Keithley Model 600A electrometer.

The illumination of the injecting electrode was achieved using the light from a mercury lamp, (Osram HBO 100 W/2). This light was passed through either a Corning Color filter #CS 5-74, (λ_{max} = 4360A°) or through a Corning Cut-off filter #CS 3-72 which cuts-off at 4300A° or through a #CS 3-70 which cuts-off at 4900A°. As is shown in Fig. 1 the path of the light, after leaving the filter, is through the conducting glass and crystal and then into the NaI-I_2 solution.

SECTION IV. EXPERIMENTAL RESULTS

Typical current-voltage characteristic curves on a log i vs log V plot are shown in Fig. 2. The changing parameter in these curves is the concentration of the iodine in the NaI-I_2 solution. The values of each curve are the average values gotten from many successive measurements on a crystal. Measurements taken on a large number of similar crystals give similar results. In all the measurements represented in Fig. 2 the electrodes were not illuminated. From measurements of this type it was found that the iodine concentration most convenient for our measurements is a 25% dilution.

No detectable changes were obtained after irradiating the crystals with the neutron sources indicated in (a) and (b) of Section II using the doses indicated in this section.

Fig. 3 represents the space charge limited currents in a log i vs log V plot with and without illuminating the injecting electrode. The iodine concentration of the injecting electrode for all our measurements was 25% of the saturated value. As shown in Fig. 2 the reproducibility is good using this concentration. Curve #I of Fig. 3 shows the results obtained when the crystal was not illuminated. Curve #II shows the results obtained when the injecting electrode was illuminated through the Corning Color filter #CS 5-74, which has a maximum transmission at λ = 4360°. Curves #III and #IV show the results obtained when the injecting electrode was illuminated through the Corning Cut-off filters #CS 3-72, (cut off at λ = 4300A°), and #CS 3-70 (cut off at λ =4900A°), respectively. The relative displacements of these four curves are explained by the fact that the light is partially absorbed by the crystal and part by the injecting iodine electrode.

As previously stated the injecting electrode was illuminated with light from a high pressure Hg source,* and as shown in Fig. 1 passes first through the color or cut-off filter then through the crystal and then is absorbed by the electrode. The displacement of curve II of Fig. 3, in which the color filter was used, from curve I, taken in the dark, in the

* intensity with filter #CS 5-74 170 μwatt/cm^2

region below the saturation current, is explained by the fact that part of the light transmitted by this filter is absorbed by the anthracene crystal. This results in a redistribution between the free and trapped carriers producing higher current values for the same voltages. The higher saturation values in the illuminated cases,[8] is due to the absorption of the light in the iodine solution near the crystal surface increasing the concentration of the disassociated iodine.

In curve III, taking account of the absorption coefficient of the anthracene and the transmission of the cut-off filter used, less light is absorbed in the crystal than in curve II resulting in a smaller displacement compared to the dark current curve. However, the saturation value of the current of curve III is greater than that of curve II because more light is absorbed in the iodine since the cut-off filter, CS 3-72, transmits all the long wavelengths of the source which are absorbed in the iodine, and also there is less light absorbed in the anthracene. The cut-off filter used for curve IV cuts off at a longer wavelength than that used for curve III, and taking into account the spectral distribution of the source explains the relative position of this curve.

Fig. 4 shows the steady state space charged limited dark current-voltage curves for a crystal before and after gamma irradiation. The parameter for these curves is the time of exposure to the gamma ray source. It is seen that, after irradiation, the slope of the curve at low

low current values is smaller than at higher current values. For high irradiation doses this slope at low current values is two. This square law extends to larger voltages the longer the time the crystal is irradiated. It is also seen that the saturation current, which is almost the same in all the curves, occurs at higher voltages when the irradiation time is longer. The curves in Fig. 5 were taken on a crystal which was irradiated with gamma rays for 3 hours. Curve I is the dark current and curves II, III and IV were taken under illumination of intensity of 25, 50 and 100% respectively.

Fig. 6 shoes the results of measurements taken on a crystal after irradiating with x-rays. As is seen the curves of Fig. 6 are similar to those of Fig. 4.

SECTION V. THEORY OF SPACE CHARGE LIMITED CURRENTS

It is well known that defects of solids produce changes in the optical and electrical properties of solids. Thus the measurement of these properties yields information about these defect states. In order to make practical electrical measurements in insulators one must enhance the free carrier density. One way of doing this is by injecting free carriers into the insulator. The current will then be limited by the space charge injected into the crystal. The steady state current for ideal crystals, as discussed by Mott and Gurney,[16] depends on the square of the applied voltage and is inversely proportional to the

cube of the crystal thickness. The theory of the steady state space charge limited current in real crystals was given by Rose[4] and Lampert[5]. From the measurement of the SCLC in crystals with traps at a discrete energy level, the trap density and depth can be computed. The theory of the transient space charge limited current for the case of an ideal crystal was first given by Many, Simhony, Weisz and Levinson[6] and independently by Helfrich and Mark[17]. The theory of the transient space charge limited current for real crystals was given by Many and Rakavy[9]. From transient measurements of the SCLC it is possible to compute the mobility and the trapping time of the carriers. These results combined with those of the steady state enables one to compute the capture cross-section of the traps. Hence, the measurement of the space charge limited current in insulators is a powerful tool in determining the characteristics of defects. Since in this report the results of steady-state space charge limited current measurements are given, a brief review of the theory for the steady-state is presented below.

Following Lampert derivation, the equations governing the steady state current flow in a one dimensional plane geometry crystal, are the following:

Eq. 1 $$J = q\mu n(x) E(x) - q D \frac{d}{dx} n(x) = constant$$

Eq. 2 $$\left(\frac{\epsilon}{q}\right)\frac{dE}{dx} = \left[n(x) - \bar{n}\right] + \left[n_t(x) - \bar{n}_t\right]$$

where $n(x)$ and $n_t(x)$ are in quasi-equilibrium.

The J is the current density; E is the electric field intensity; q is the magnitude of the electric charge; μ is the electronic mobility; ϵ is the static dielectric constant of the insulator; D is the diffusion constant for electrons; $n(x)$ and $n_t(x)$ are the densities of the free and trapped electrons respectively; and $\bar{n}$ and $\bar{n}_t$ are the values of n and n_t respectively in the bulk neutral crystal in thermal and electrical equilibrium, (that is, no applied voltage).

In solving these equations the diffusion term in Eq. 1 is neglected, which is reasonable for voltages greater than $\frac{kT}{q} = 0.025$ volts. The solution to these equations for the ideal crystal, (no traps), with the boundary condition $E = 0$ at $x = 0$ was given by Mott and Gurney by substituting the expression for n in Eq. 2 into Eq. 1 and integrating with the above boundary condition. The result for J is,

Eq. 3 $$J = \frac{9}{8}\epsilon\mu\frac{V^2}{L^3}$$

where V is the applied voltage and L is the crystal thickness.

Lampert gave the exact solution for a crystal containing traps at a single energy level for the case where $\frac{E_t - E_a^F}{kT} > 1$, where E_t is

the trap level energy as measured from the bottom of the conduction band and $\mathcal{E}_a^F$ is the Fermi-level of the crystal at the anode. In this case the current is diminished by a factor θ compared to the ideal case, (Eq. 3), and is given by:

Eq. 4 $$J = \frac{9}{8} \epsilon \mu \theta \frac{V^2}{L^3}$$

where θ is,

Eq. 5 $$\theta = \frac{n_c}{n_t} = \frac{N_c}{N_t} \exp\left(-\frac{\Delta \mathcal{E}_t}{kT}\right)$$

where $\Delta \mathcal{E}_t$ is the magnitude of the trap depth, and N_c and N_t are the densities of available states in the conduction band and traps respectively. When the voltage is such that all the traps are filled a sharp rise in the current occurs and the value given by Eq. 3 for the ideal case is reached.

Lampert showed that the current-voltage characteristics curves when plotted on a log J versus log V plot will be confined to lie in a triangle as shown in Fig. 7. For voltages less than $V^{(\Omega-C)}$ the current will follow Ohm's Law because the number of injected carriers n(x) is less than $\bar{n}$, the number of free carriers in the absence of injection. For voltages greater than $V^{(\Omega-C)}$ in a trap free crystal, the current will obey Child's Law as given by Eq. 3. In the case of a real crystal the departure from Ohm's Law will occur at a higher voltage due to the fact that only a fraction of the total injected carriers is free. If all the

traps are at a single energy level the current will again follow a V^2 law but will be below the Child's Law by a factor θ as given by Eq. 5. At the voltage, V^{TFL}, when the number of injected carriers is approximately equal to the number of traps in the crystal, a large rise in the current occurs for small increases in voltage until the Child's Law value is reached. For higher voltages, since all the traps are filled, the injected carriers see an ideal crystal and Child's Law is followed.

For crystals which contain trap levels that are distributed in energy, θ will no longer be a constant but rather a function of the voltage. In these cases, when the current departs from Ohm's Law it will follow a voltage dependence $J \sim \theta(V)V$. One can see that from a simple steady state current-voltage measurement made on an insulator with an injecting electrode a large amount of information can be ascertained. By taking the ratio of the experimental value to the ideal Child's Law value for the current θ is evaluated. From the voltage dependence of θ the energy distribution of the trap levels can be determined. From the V^{TFL} value the trap density, N_t, can be evaluated. In the case where θ is not a function of the voltage the energy depth of the traps can be found by using Eq. 5.

SECTION VI. CONCLUSIONS

As is seen in Fig. 4 the current-voltage curve is effected by the gamma radiation in such a way that for a given voltage the current value is lowered. The larger the radiation dose, that is, going from curves II to V, the lower is the current. There is also a change in the slope. Beginning with curve II the current at low voltages departs from a v^n dependence, where $n > 2$, to a V^2 dependence. In curve V a V^2 dependence holds till the breakdown voltage. For higher radiation doses the currents are lower than in curve V but the V^2 dependence still holds.

These curves are interpreted in terms of the space charge limited theory. Results similar to curve I, the measurements made on the thin anthracene crystal before irradiation, have been reported by Mark and Helfrich[8]. These curves can be explained in terms of an exponential trap distribution. The lowering of the current value for a given voltage going from curves II to V, are interpreted in terms of traps which are created by the radiation. As N_t, the density of traps is increased, the number of free carriers at a given voltage is decreased. The gradual change in the slope to a value of 2 for higher radiation doses strongly indicates that the traps introduced by the radiation are all at the same discrete energy level. Using the equations of the space charge limited current theory outlined in Section V, the parameters of these traps can

be calculated. From curve IV of Fig. 4, the value of the voltage where the curve departs from a square law dependence is seen to be about 200 volts. Taking this to be the value of the trapped filled limit voltage for the introduced traps and using this value in the equation, $V^{TFL} = \frac{q L^2 N_t}{2\epsilon}$, where L is the crystal thickness, q the electronic charge, and ϵ the dielectric constant, N_t, the trap density, is calculated to be $2 \times 10^{13}/cm^3$. From the ratio of the current of curve IV and the ideal V^2 curve, the ratio, θ, is $\approx 10^{-8}$. Using Eq. 5 and $N_t = 10^{13}/cm^3$ and taking N_c, the number of states in the conduction band to be $10^{21}/cm^3$, the value of ΔE, the trap depth, is found to be 0.92 ev.

From curve I of Fig. 4 it is seen that a saturation value of the current is reached. As is seen from curves II and III this saturation value is not effected by the radiation. However, the voltage at which saturation occurs depends on the radiation dose, that is on the number of traps introduced. The reason for this is that as the number of traps is increased the number of free carriers is decreased at any given voltage. The electrode injection, which in the steady state is dependent on the number of free carriers, will in the case of greater trap density, hold for higher voltages. For the higher radiation doses, curves IV and V, a breakdown occurs before the current saturation is achieved. In Fig. 5 the light intensity dependence of the current is shown for a crystal where a large number of traps has been introduced. Curve I of Fig. 5 was taken with a crystal in the dark, and curve II was taken when the

crystal was illuminated by light which passed through filter CS 3-70, (cut-off at 4900A°). Taking this light intensity as 100%, curves III and IV were measured at intensities of 50% and 25% respectively.

The results taken on a crystal exposed to 120 kvp x-rays is shown in Fig. 6. The time of irradiation differs for each curve and was adjusted so that the total amount of energy absorbed in the crystal was the same as the equivalent curves for the gamma radiation shown in Fig. 4. It is seen that qualitatively and quantitatively the curves are similar.

Our work so far shows that anthracene crystals are damaged by radiation from gamma and x-rays and that this damage can be detected by electrical conductivity measurements. This type of measurement can be used to measure the magnitude of the damage but does not provide information about the nature of the damage. We hope that the experiments we have planned for the future will enable us to obtain information concerning the nature of the damage.

BIBLIOGRAPHY

(1) KOMMANDEUR, J.: Ph. D. Thesis, University of Amsterdam (1958)

(2) KOMMANDEUR, J., and SCHNEIDER, W.A.: J. Chem. Physics, 28 590 (1958)

(3) KALLMANN, H., and POPE, M.: J. Chem. Physics 32, 300 (1960)

(4) ROSE, A.: Phys. Rev. 97, 1538, (1955)

(5) LAMPERT, M.A.: Phys. Rev. 103, 1648 (1956)

(6) MANY, A., SIMHONY, M., WEISZ, S.Z., and LEVINSON, J.: J. Phys. Chem. Solids, 22, 285 (1961)

(7) SILVER, M. et al,: J. Phys. Chem. Solids 23 419, (1962)

(8) MARK, P., and HELFRICH, W.: J. Appl. Physics 33, 205 (1962)

(9) MANY, A., and RAKAVY, A.: Phys. Rev. 126, 1980 (1962)

(10) MANY, A., WEISZ, S.Z. and SIMHONY, M.: Phys. Rev. 126 1989 (1962)

(11) WEISZ, S.Z. et al,: J. Chem. Phys. 40 3365 (1964)

(12) MANY, A., SIMHONY, M., WEISZ, S.Z., and TEUCHER, Y.: J. Phys. Chem. Solids 25 721 (1964)

(13) KALLMANN, H. and POPE, M.: Rev. Sci. Inst. 30, 44 (1959)

(14) KALLMANN, H. and POPE, M.: Rev. Sci. Inst. 29, 993 (1958)

(15) NBS HANDBOOK #63

(16) MOTT, N. F. and GURNEY, R.W.: Electronic Processes in Ionic Crystals (Oxford University Press, N. Y. 1940 p. 172).

(17) HELFRICH, W. and MARK, P.: Z. Physik 168 495 (1962)

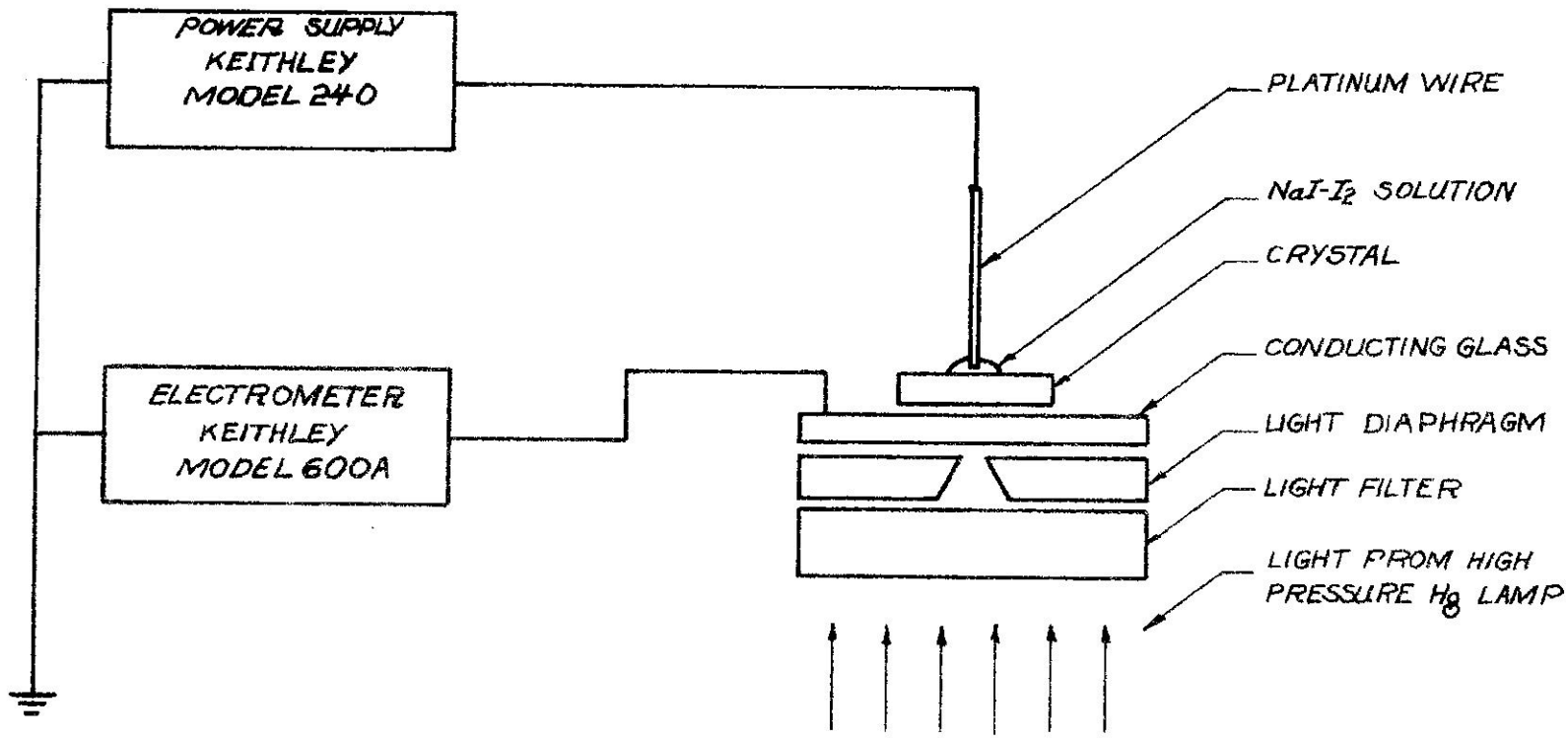

Fig. 1. Block Diagram of the Experimental Apparatus.

Fig. 2. Typical Dark Current-Voltage Characteristic Curves for Different Iodine Concentrations

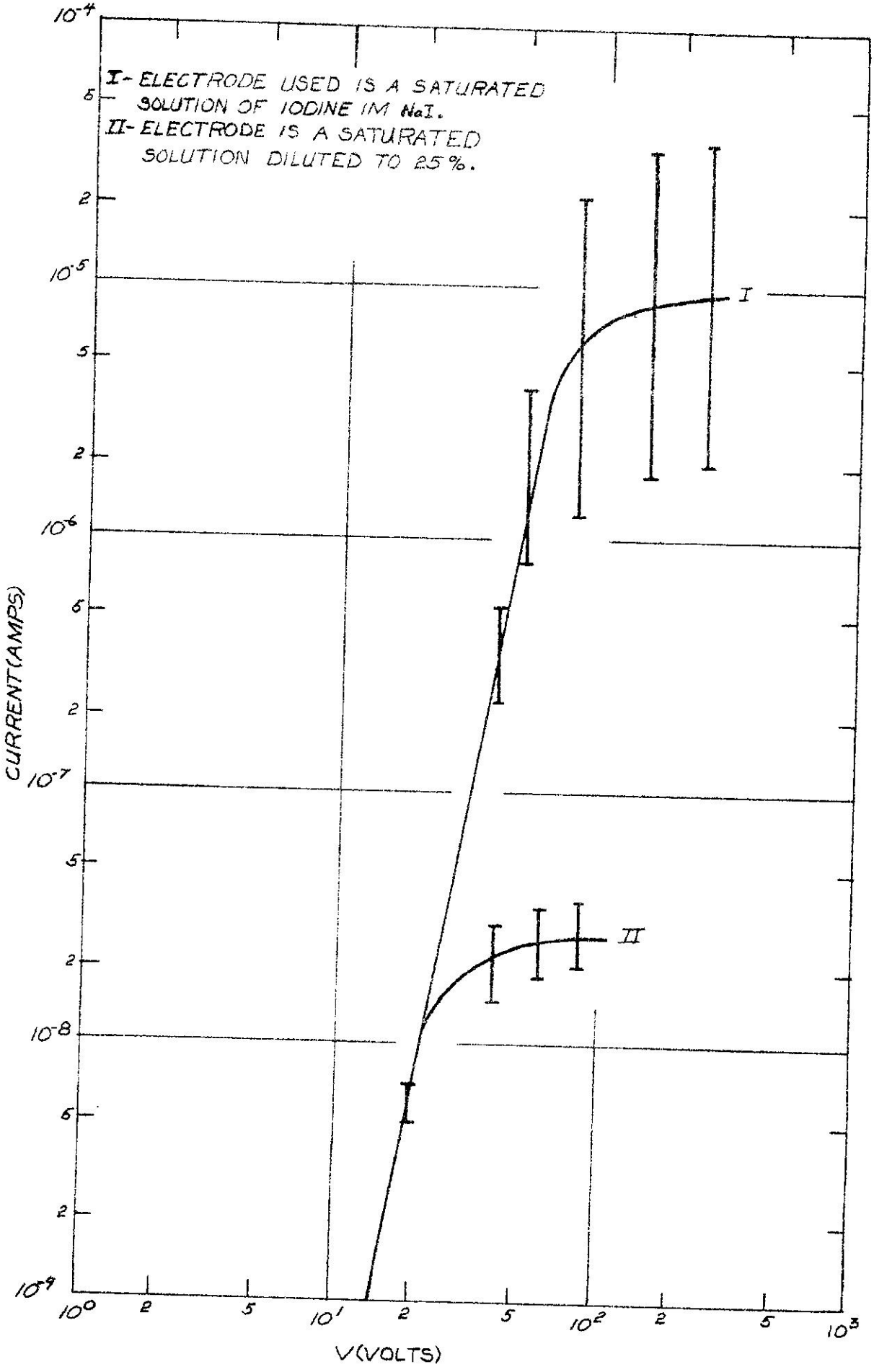

Fig. 3. Current-Voltage Curve for a Crystal in the Dark and under Illumination with Various Filters

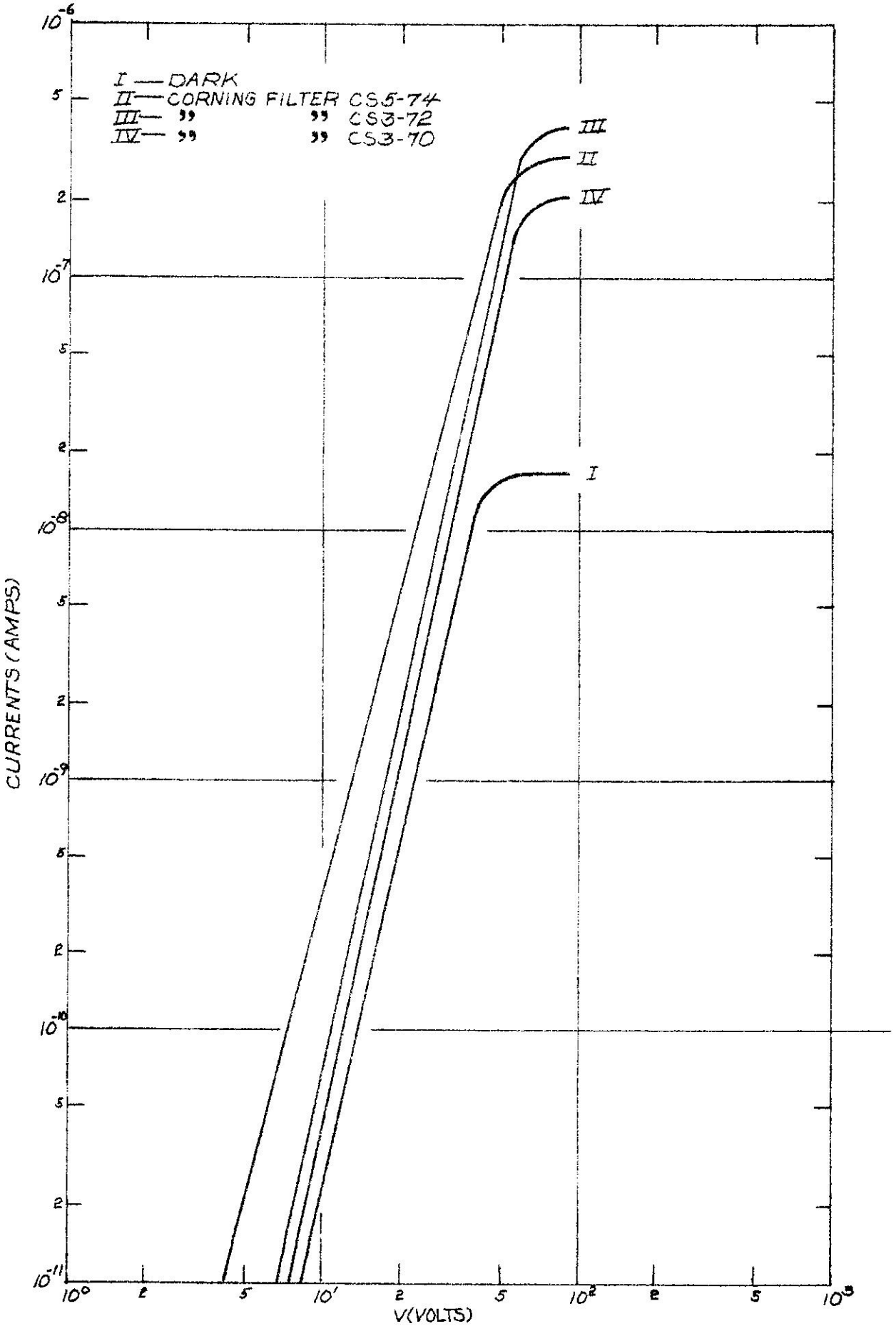

Fig. 4. Dark Current-Voltages Curves of a Crystal before and after Exposure to Gamma rays for Different times.

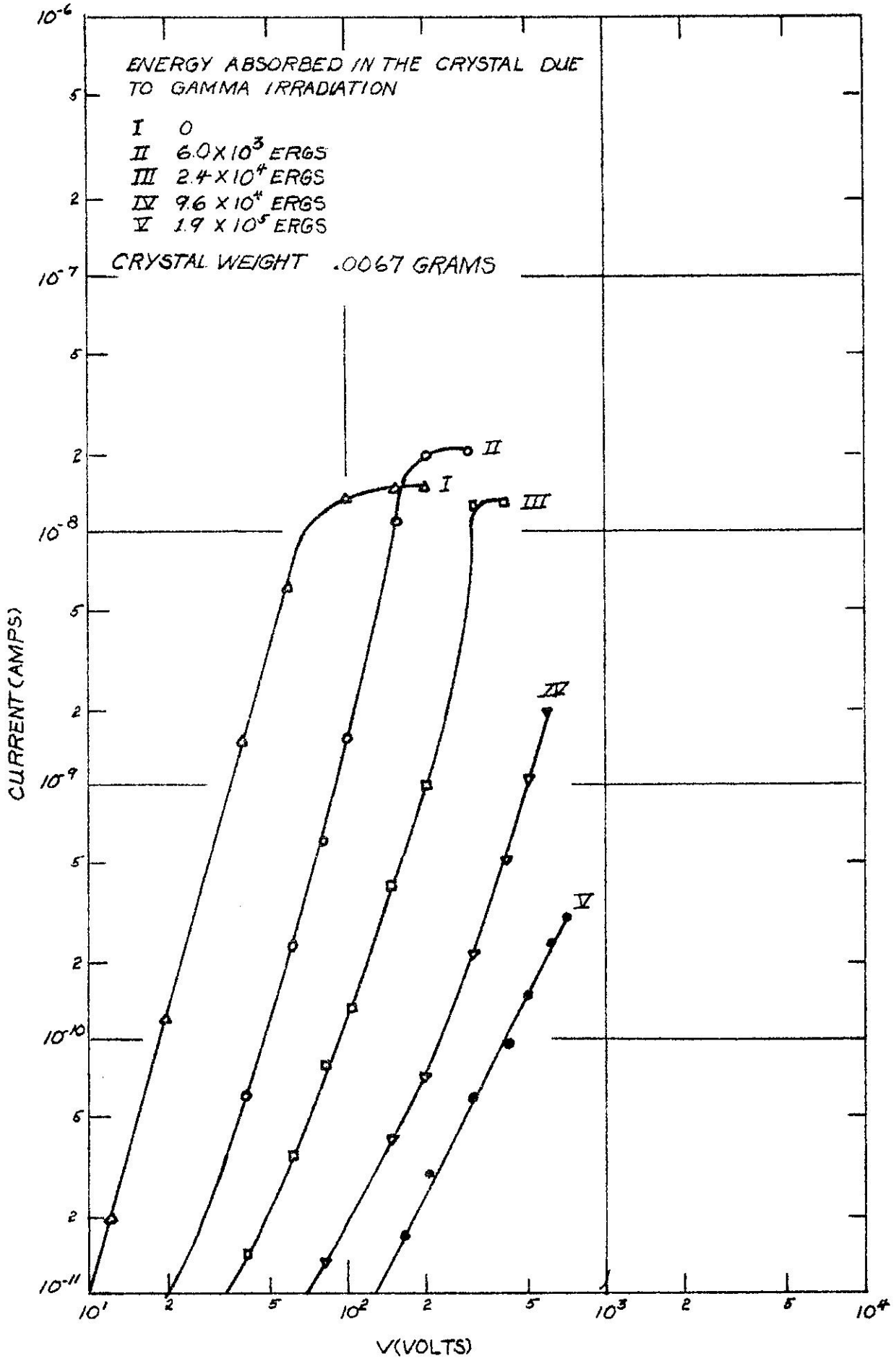

Fig. 5. Current-Voltage Curves as a Function of Light Intensity for a Crystal which was Exposed to a High Gamma ray Radiation Dose.

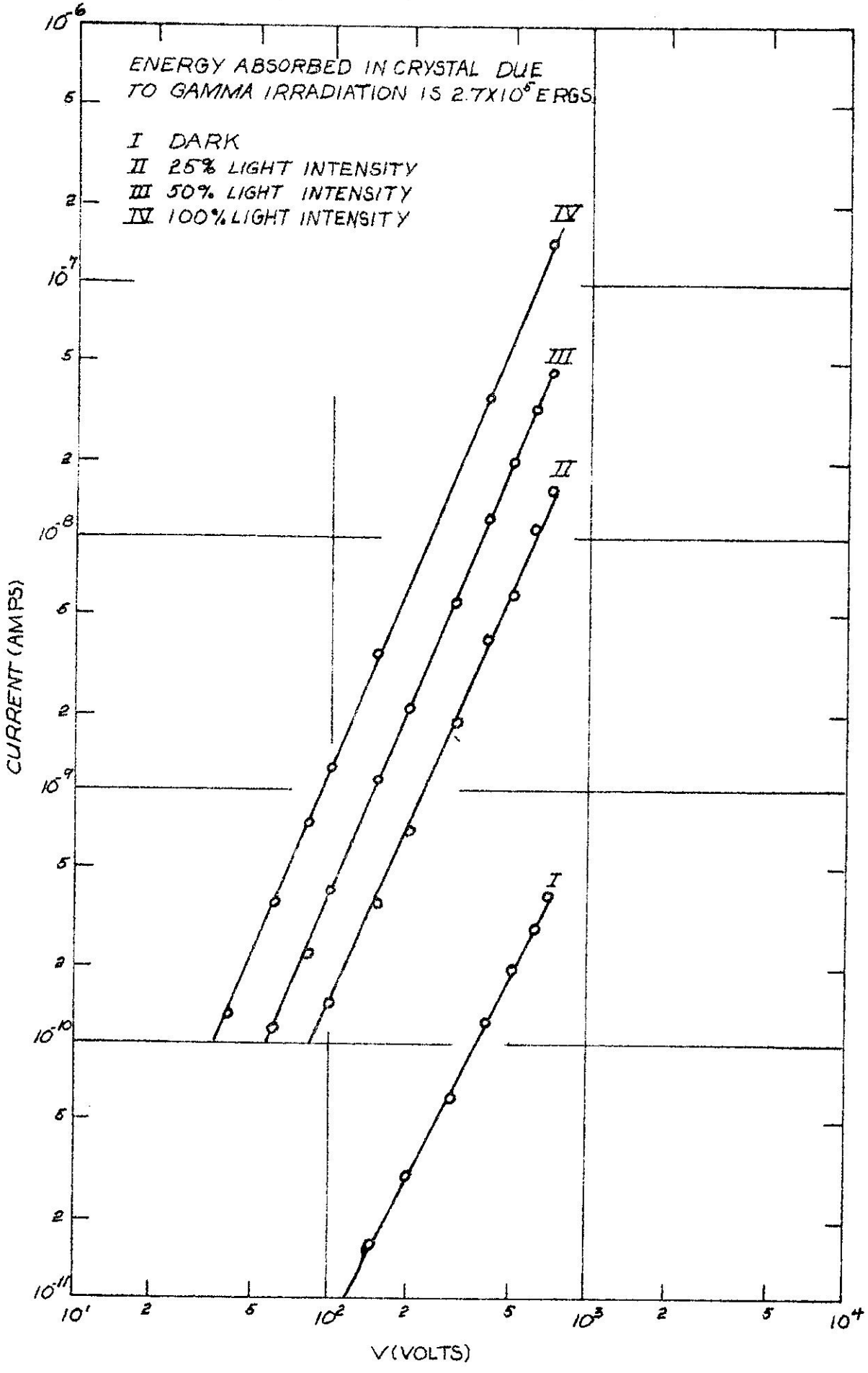

Fig. 6. Dark Current-Voltage Curves of a Crystal before and after Exposure to X-rays for Different times.

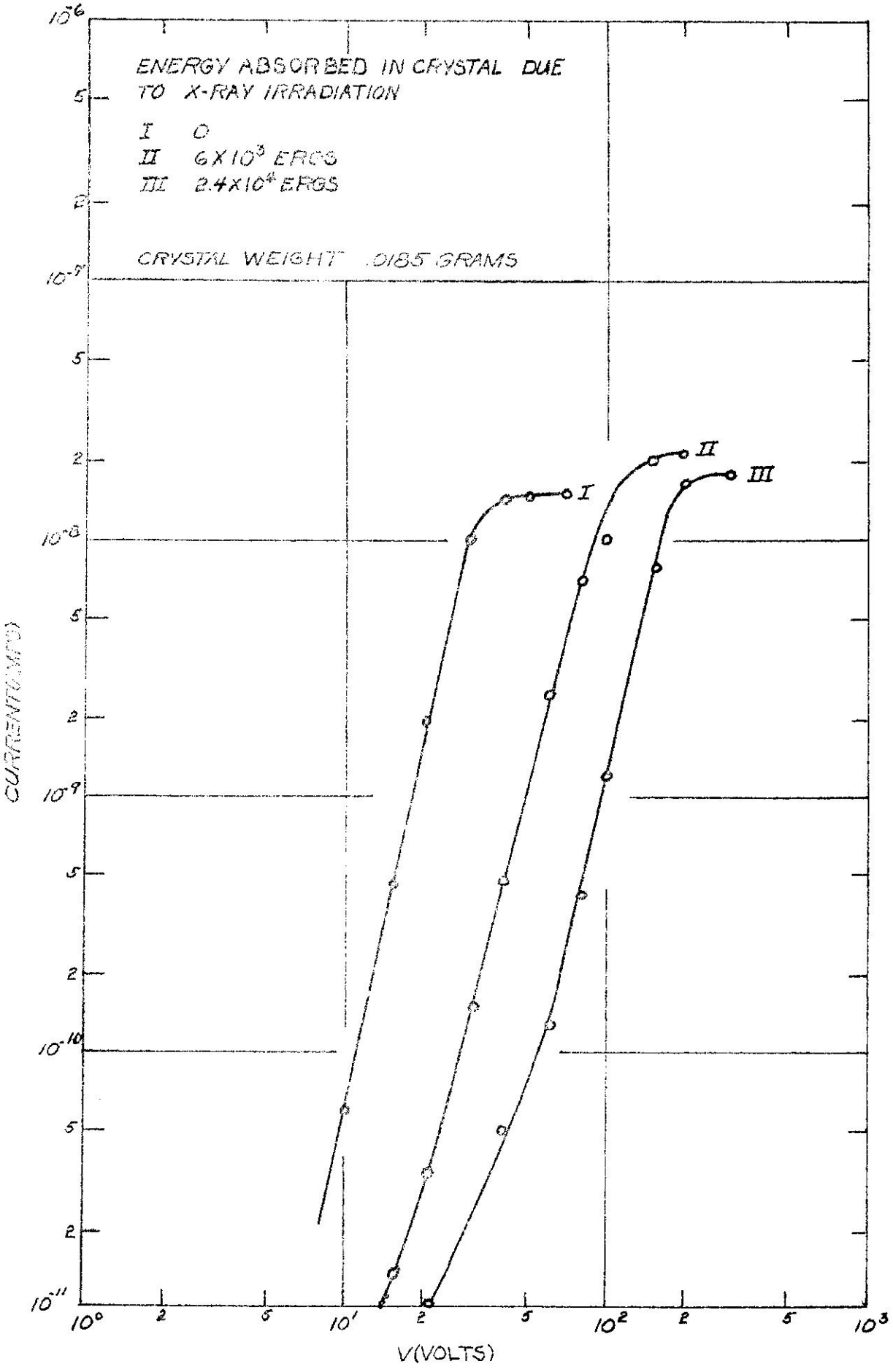

Fig. 7. Triangle Defining the Limited of the Space Charge Limited Current.